J. Fluid Mech. (1975), *vol.* 71, *part* 4, *pp.* 769–784
Printed in Great Britain

A model for the axial decay of a shock wave in a large abrupt area change

By S. A. SLOAN AND M. A. NETTLETON
Central Electricity Research Laboratories, Kelvin Avenue, Leatherhead, Surrey, England

(Received 2 July 1974 and in revised form 25 March 1975)

A shock–dynamic model based on the symmetrical expansion of the critical shock is used to analyse the progressive decay of an originally planar shock wave through a large and abrupt area change. This is tested against measurements of shock strength made along the axes of area changes where the shock waves are free to expand in two or three dimensions.

The critical shock is defined as the configuration when the decaying shock wave at the axis first becomes curved. The axial shock begins to decay less than one diameter from the entrance of the area change. Differences between the experimental onset of decay and the theoretical position of the critical shock are accounted for by the non-ideal behaviour of a practical pressure transducer.

The model predicts that, when the shock wave is decaying symmetrically, there is a linear relationship between a derived function ϵ of the decaying shock strength and the distance from the area change. This is confirmed experimentally for all the shocks studied. The quantitative application of the results in three dimensions up to 400 mm enables accurate predictions of experimental results at 1 m for $M < 2{\cdot}0$. Also, the model may be applied to three-dimensional results to predict accurately equivalent results in two dimensions.

The numerical values of ϵ are based on the equivalence of the ratio of the shock areas and the ratio of their Chisnell (1957) functions. Hence correlations between experimental results and predictions of the model are evidence that Chisnell's theory can be extended to include large and abrupt area changes.

1. Introduction

Chester (1953, 1954) developed an analytical treatment for the motion of a shock wave along a gradually diverging duct. This was based on linearization of the hydrodynamic equations and is only strictly valid for small area changes.

Chisnell (1957) integrated Chester's equations and derived in closed form a relationship between the cross-sectional area of the channel and the pressure ratio of the resultant shock wave. This was used to determine the quasi-steady pressure level in the exit channel of a small and gradual area change simply from

$$Af(Z) = A'f(Z'), \tag{1}$$

where A and A' are the cross-sectional areas of the entrance and exit ducts respectively and $f(Z)$ and $f(Z')$ are the Chisnell functions appropriate to the incident and decayed shock waves.

The extension of the Chester–Chisnell treatment to predicting unsteady pressures following and within area changes which are not small is a source of controversy. Davies & Guy (1971) used Chisnell's relationship in their stepwise model for the unsteady shock strength. They compared experimental and theoretical results for area changes of 4 : 1 and 10 : 1 and found the correlation satisfactory only for the smaller ratio. Deckker & Gururaja (1970) have examined the decay of a shock wave in a diffuser and concluded that Chisnell's analysis was unsatisfactory.

Since the Chester–Chisnell method is such an important tool in the theoretical treatment of expanding shock waves, it would be useful to know the limits of its application. To this end Nettleton (1973) studied the effect of the angle of divergence and the magnitude of the area ratio (up to 5·0) on the attenuation of a shock wave in a two-dimensional expansion. He concluded that, for a shock wave with an initial Mach number less than 3·0, the Chisnell analysis adequately predicted the quasi-steady shock strength 5 diameters downstream of the area change for divergence angles up to 15°.

Whitham (1957, 1959) approached the problem of expanding shock waves from the theory of characteristics. He introduced the concept of rays, which basically are the trajectories of points on the wave front and as such are necessarily orthogonal to the shock wave at the point of contact. His treatment of the propagation of an element of the shock wave along a narrow tube of neighbouring rays was based on an analogy with the propagation in a solid tube of smoothly varying cross-section. It was assumed that the local Mach number M of the shock wave and the area A of the ray tube were functionally related by Chisnell's relationship. Skews (1966) used Whitham's theory in his quantitative description of shock diffraction.

The results reported in § 3 are for the incident shock strength along the axis as an originally planar shock wave was allowed to expand through a large and sudden area change. Area changes both of circular and of rectangular cross-section were studied, and the results are alternatively referred to as three- and two-dimensional or as having three and two degrees of freedom respectively. The shock waves eventually acquired spherical or cylindrical symmetry. In each case the side wall was at an angle of 90° to the axis, giving an abrupt change in cross-section. The parallel walls of the larger duct were so distant that waves reflected from them did not affect the measurements. Thus each area change was effectively a half-space.

The incident shock strengths were obtained from reflected-shock profiles. This was necessary in the three-dimensional experiments since it was not feasible to measure directly the pressure of a decaying incident shock. In the two-dimensional case, it was chosen because it allowed measurements at any position and required only one gauge calibration. In contrast, James (1965) measured shock strengths both along the axis and at angles of from 30° to 150°, with a series of gauges. The interaction of the shock wave with the leading gauge is likely to affect the results at subsequent gauges. Interference of reflexions from the ground (about 1 m from the axis) precludes generalization of James' results.

In § 4 a model for the decay of the shock is developed, based on a two-stage

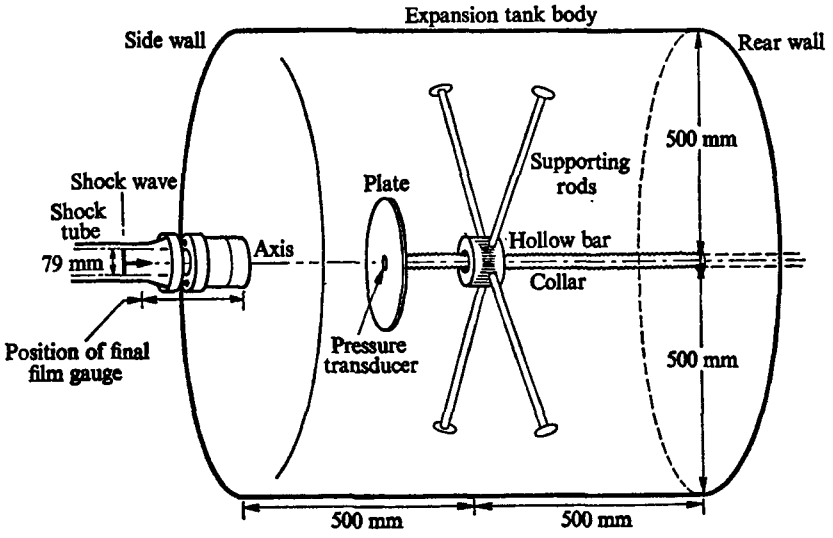

FIGURE 1. Expansion tank and reflecting plate.

process. The first is diffraction, during which no attenuation occurs along the axis. The shock configuration at the completion of this is defined as the critical shock. The second stage is the expansion of this critical shock, which eventually attains either spherical or cylindrical symmetry. Chisnell's (1957) equations are used to quantify the model in terms of ϵ, which is a measure of shock decay. It is found that soon after the critical shock position ϵ is a linear function of the axial distance. Such linear relationships allow transformation of the results from three dimensions to predict accurately the results in two dimensions. In § 5 it is argued that Chisnell's theory can be extended to include unsteady shock decay in a half-space, provided that the initial conditions are defined in terms of the critical shock configuration.

2. Experimental

The three-dimensional results were obtained when an originally planar shock wave in a cylindrical shock tube of diameter 79 mm was allowed to expand into a cylindrical tank of diameter 1 m (figure 1). To obtain pressure histories a Kistler 601 A pressure transducer was located axially within the tank in a reflecting plate of diameter 200 mm. Thus, on the axis, the face of the transducer was normal to the shock flow. The plate was placed at distances up to 450 mm from the entrance of the tank. The output from the transducer was amplified by a Kistler 566 charge amplifier and displayed on a Tektronix 556 oscilloscope fitted with a filter to attenuate frequencies above 30 kHz. This was required to reduce the contribution to the signal of resonant ringing of the transducer. The portion of the profile before the peak occurring 11 μs after shock reflexion was not reproducible. The transducer/plate assembly was calibrated for this peak (indicated by the arrow in figure 2) by reflecting shocks of known strength from the

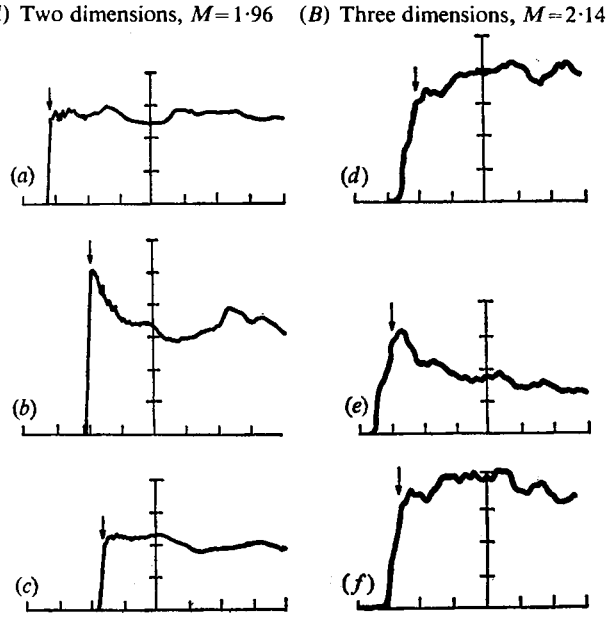

FIGURE 2. Typical pressure histories. All divisions on abscissae 20 μs.

	X (mm)	χ	Ordinate scale (N m^{-2} div^{-1})		X (mm)	χ	Ordinate scale (N m^{-2} div^{-1})
(*a*)	2	0·09	4×10^4	(*d*)	2	0·025	8×10^4
(*b*)	17·3	0·79	2×10^4	(*e*)	58	0·73	8×10^4
(*c*)	147	6·68	1×10^4	(*f*)	275	3·48	8×10^3

plate with the plate at a distance of 2 mm from the entrance to the area change, and a linear calibration was obtained from 1·4 to 5·0 bar. This was extrapolated to the origin and used to determine the overpressure due to reflexion of a decaying shock front as the plate was moved away from the entrance to the area change. Figure 2 (*B*) shows typical pressure histories.

The apparatus for the two-dimensional experiments was similar. A planar shock wave from a rectangular shock tube (47 × 22 mm) was vented into a parallel-sided 90° expansion tank of cross-section 47 × 340 mm. The laterally expanding shock wave was reflected from a rectangular plate (44 × 200 mm) in which was located axially a Kistler 603 B pressure transducer. This acceleration-compensated transducer had a higher frequency response (400 kHz compared with 150 kHz) which was only partly negated by the 150 kHz frequency response of the charge amplifier. Thus it was possible to obtain acceptable results using the peak occurring only 3 μs after shock reflexion (indicated by the arrow in figure 2 *A*). The pressure profile (figure 2 *A*) was recorded without use of the frequency filter on the oscilloscope. The calibration graph was linear over its entire range (0·58–1·7 bar) and was extrapolated to the origin as before. Pressure histories were obtained with the reflecting plate at distances up to 280 mm from the entrance of the tank.

Pressure histories were also obtained when the shock wave was reflected from a transducer mounted axially on the rear wall of the cylindrical tank (X = 1 m).

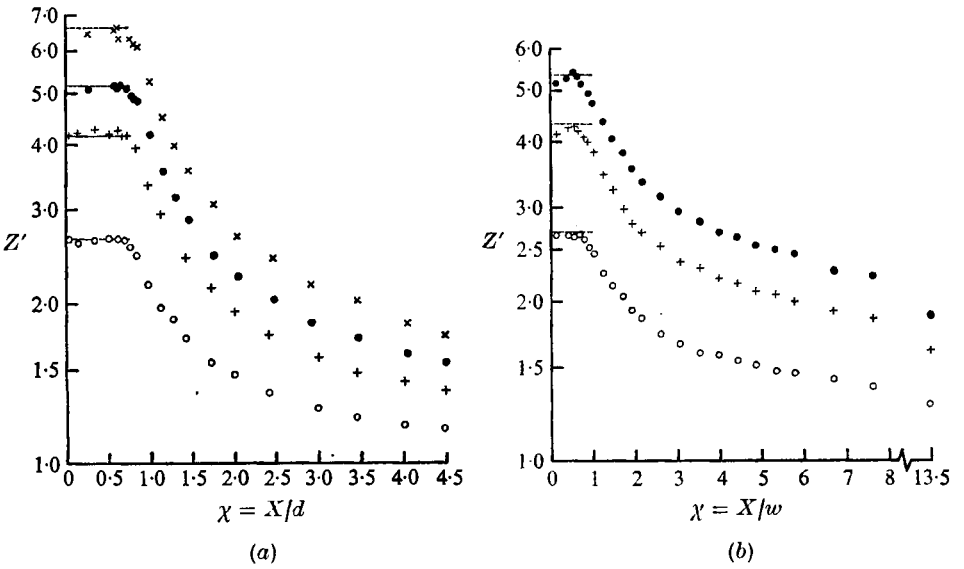

FIGURE 4. Axial shock strength of incident shocks expanding with (*a*) three and (*b*) two degrees of freedom.

		○	+	●	×
(*a*)	*M*	1·55	1·92	2·14	2·42
(*b*)	*M*	1·57	1·96	2·18	

Since this transducer was solidly mounted no special calibration was required. These experiments were carried out in the absence of the reflecting plate.

Single-shot schlieren photographs (figure 3, plate 1) of a decaying shock wave of initial Mach number 1·5 were obtained using an argon jet light source of sub-microsecond duration. In order to model the side wall, the cylindrical tank was replaced by a smooth annulus of diameter 1 m coaxial with and of the same bore as the shock tube.

3. Results

In order to compare the experimental results for the two geometries it is necessary to define a non-dimensional distance co-ordinate χ. This is the axial distance divided by either the diameter d of the cylindrical shock tube or the width w (22 mm) of the shock tube of rectangular cross-section, as appropriate.

Primed quantities are used throughout to denote parameter values after the shock wave has entered the area change.

Pressure histories (figure 2) were obtained from shock waves propagating through air in the expansion tanks of cylindrical or spherical symmetry. Using the calibration graphs and the standard equation connecting the pressures on either side of a reflected shock, the height of the appropriate peak gave the pressure ratio Z' of the decaying incident shock. Figures 4 (*a*) and (*b*) show Z' as a function of χ as the reflecting plate is moved away from the entrance to the area change. The results from the cylindrical shock tube (figure 4*a*) were reproducible

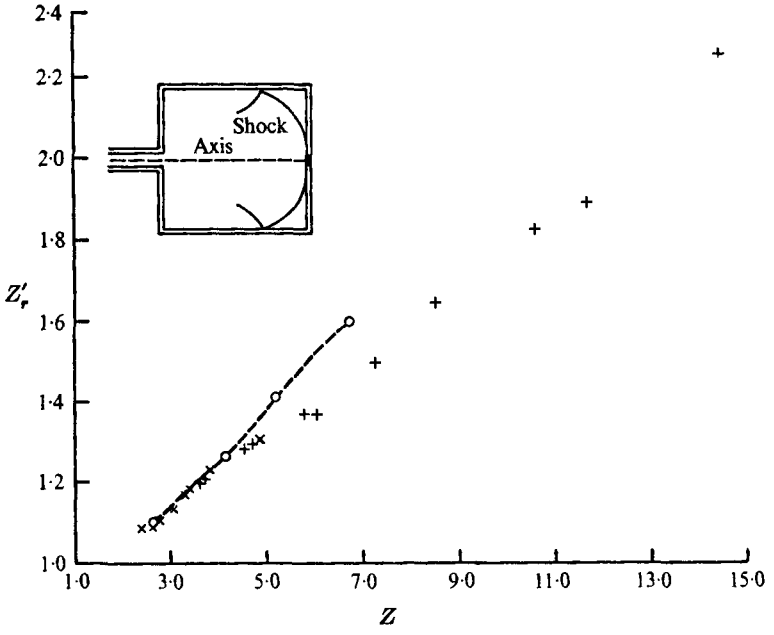

FIGURE 5. Reflected-shock strength at $\chi = 12{\cdot}7$ for three degrees of freedom. ×, air driven; +, He driven; ○, extrapolated from results up to $\chi = 4{\cdot}5$.

to within a few per cent and only one run was required for each position of the plate. The fluctuations in the two-dimensional results were much larger and each point in figure 4 represents the mean of values of Z' from three runs. The initial shock Mach numbers in the two-dimensional system were 1·57, 1·96 and 2·18. These are comparable to the Mach numbers of 1·55, 1·92 and 2·14 in the three-dimensional experiments, which also produced results for a Mach 2·42 shock. The characteristics of the two shock tubes were such that the spread of the initial Mach number within a series of runs with the cylindrical tube ($\pm 1\%$) was about doubled when the rectangular tube was used, and this contributed to the fluctuations in the results obtained for each position of the plate.

Plots such as figures 4 (*a*) and (*b*) suggest that the expansion of a shock within an area change occurs in two phases. The axial shock strength remains roughly constant before decreasing rapidly. Each horizontal line corresponds to the pressure ratio Z of an undecayed shock of the appropriate mean initial Mach number. These correlate well with the plateaus in figures 4 (*a*) and (*b*), indicating that the shock must travel a significant distance before it weakens on the axis.

This is supported by figure 3, which shows a series of schlieren photographs of a Mach 1·5 shock wave progressively decaying in a three-dimensional half-space from an almost planar shock in (*a*) to a completely curved shock in (*h*). It should be noted that the axial (central) segment of the decaying shock remains planar for a considerable portion of its travel. While the axial part of the shock is planar, it has not been weakened, resulting in the plateaus in the pressure ratios shown in figures 4 (*a*) and (*b*).

Reflected pressure ratios Z'_r at $\chi = 12{\cdot}7$ are shown in figure 5 for both air- and helium-driven shocks. Within the experimental error Z'_r is considered to be a linear function of the initial shock strength. Z'_r must asymptotically approach unity, since the shock will eventually decay to a sound wave. However, even with initial shock strengths as low as 2·3, significant reflected shock pressures were recorded at $\chi = 12{\cdot}7$.

4. A model of shock decay and comparison with experiment

4.1. *The model*

The most striking feature of the experimental results is the initial plateau in the plots of shock strength against distance (figure 4). Thus the process of shock decay must occur in at least two very different stages. The application of Chisnell's relationship (1) in isolation will not predict such a pressure plateau.

It is obvious from the schlieren photographs in figure 3 that the full description of shock decay involves the diffraction of the shock at the entrance to the area change. When a shock wave passes a convex corner an expansion wave is propagated radially through the flow behind the shock. This wave travels with the local velocity of sound relative to the gas. When the appropriate component of the gas velocity is added, the resultant wave becomes elongated in the direction of the flow. By considering the relative velocities of the expansion wave and the incident shock wave, Skews (1967) showed that the trajectory of the point of contact between the shock and the expansion wave was linear and inclined at an angle α to the original direction of the flow, where

$$\tan^2\alpha = \frac{(\gamma-1)(M^2-1)\{M^2+2/(\gamma-1)\}}{(\gamma+1)M^4}. \tag{2}$$

In two dimensions the shock wave is diffracted at each edge of the area change. Considering both diffractions together leads to an exact description of the expansion of the shock up to the instant that the intersections of the shock and the expansion waves from the opposite corners cross.

If the shock wave is free to expand in three dimensions, it diffracts around the rim of the entrance of the area change. Skews' equation was developed for a two-dimensional diffraction. The shape and strength of the diffracting wave is different in three dimensions, but the angle of propagation α of the intersection of the shock and expansion wave remains unchanged.

The axial segment of the shock wave cannot attenuate until the expansion wave propagating along the shock front arrives at the axis. This important configuration in the process of the shock decay is defined as the 'critical shock', which at the axis still has the same Mach number and pressure ratio as the initial shock. Equation (2) is used to determine the position of the critical shock. For correlation with the experimental results for the onset of decay (§ 4.2), this has to be modified to account for the non-ideal behaviour of the pressure transducer.

Thus the concept of the model is that the shock does not experience any decay at the axis until it becomes the critical shock, after which it expands, eventually

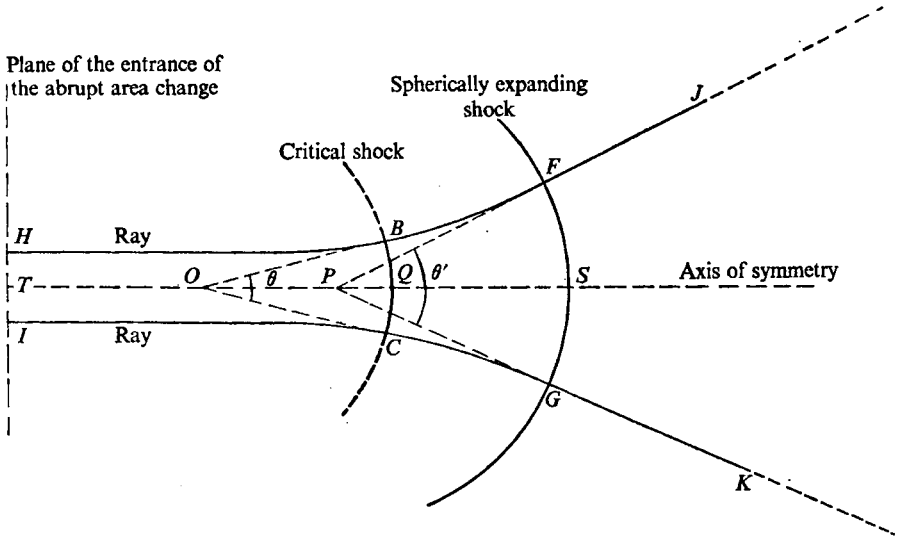

FIGURE 6. Section through the axis of the flow field of a shock expanding with three degrees of freedom.

acquiring the appropriate symmetry. The surface area of an axial segment of the critical shock is taken as the initial area A in a Chisnell–Whitham type analysis as shown in figure 6, which represents a section through the vertical axis of a small element of the flow field of a shock wave expanding with three degrees of freedom. The plane of the entrance of the tank is HTI. The shock wave first becomes non-planar at the axis at Q. The shock at Q is thus the critical shock.

The rays $HBFJ$ and $ICGK$ represent a section through a very narrow hypothetical ray tube close to the axis of symmetry. By definition rays are normal to the shock wave at all points of contact. Each segment of the shock wave within the ray tube is considered as an element of a sphere, and tangents to the rays intersect on the axis at the centre of curvature of that segment of the shock wave.

Thus the critical shock at Q has centre of curvature at O and a radius of curvature r. θ is the solid angle of the cone BOC. As the shock propagates beyond Q, its velocity, and thus the pressure ratio across it, decreases. This leads to a divergence of the rays, causing an increase in the surface area of the segment of the shock within the ray tube. While the rays remain curved, the position of the centre of curvature is changing. At some time during the decay, the rays become straight and the shock wave near the axis can be accurately described as having a fixed centre of curvature. Subsequent expansion of the shock segment within the ray tube has spherical symmetry. This is represented in figure 6 by the segment FSG centred on P. Subsequent segments of the shock expanding within the ray tube are also centred on P. Thus the solid angle θ' remains constant.

Consider now the mathematical implications of such a model. The use of displacement vectors in the analysis enables the geometric relationships to be formulated independently of changes in the relative positions of T, O, P and Q, which in figure 6 were chosen arbitrarily. Each segment of the shock is treated as

an element of a sphere, and the initial area A is equated to the surface area of the axial segment of the critical shock. Applying Chisnell's relationship (1) leads to

$$\left(\frac{A'}{A}\right)_3 = \left(\frac{\overline{PS}}{\overline{OQ}}\right)^2 \frac{\theta'}{\theta} = \epsilon_3^2, \tag{3}$$

where the subscript 3 refers to the number of degrees of freedom of the shock expansion. Separating $\overline{PS}$ into its component vectors and writing the equation in terms of χ gives

$$\epsilon_3 = \frac{d}{\overline{OQ}}\left(\frac{\theta'}{\theta}\right)^{\frac{1}{2}}\chi + \frac{d}{\overline{OQ}}\left(\frac{\theta'}{\theta}\right)^{\frac{1}{2}}\frac{\overline{PT}}{d}. \tag{4}$$

A similar argument for an expansion with two degrees of freedom gives the following equation:

$$\epsilon_2 = \frac{w}{\overline{OQ}}\frac{\alpha'}{\alpha}\chi + \frac{w}{\overline{OQ}}\frac{\alpha'}{\alpha}\frac{\overline{PT}}{w}, \tag{5}$$

where α and α' are the linear angles between the rays.

4.2. *The onset of decay*

The positions of the onset of decay were determined accurately from plots of the normalized incident shock pressure ratio Z'/Z against distance (figure 7). This reduced the scatter due to the spread in the Mach number of the initial shock and accentuated the plateau region. The plateau was determined as the best line of zero slope and its level did not vary significantly from unity. The worst case was $0{\cdot}97 \pm 0{\cdot}02$ for the Mach 1·96 shock in two dimensions. The experimental onset of decay was determined by the intersection of the plateau and the least-squares straight line through the first few points of the decay curve.

In the idealized model, the position X_0 of the critical shock at which decay begins is given by

$$X_0 = \tfrac{1}{2}w\cot\alpha \tag{6}$$

or

$$X_0 = \tfrac{1}{2}d\cot\alpha. \tag{7}$$

Whitham's (1957) theory and Skews (1967) equations provide alternative values for the angle α of propagation of the point of contact between the shock and the expansion wave, giving rise to different predicted positions for the critical shock configuration. These are compared in table 1 with the experimental distances for the onset of decay. (The results are presented in mm rather than dimensionless units because the diameter of the pressure transducer is independent of the dimensions of the shock tube.)

As can be seen, Whitham's theory predicts the critical shock to be at distances much larger than the experimental values for the onset of decay. Those predicted by Skews' theory are in better agreement, but are still far from satisfactory.

The positions of the critical shock and the onset of decay are directly comparable only if the latter is based on the instantaneous detection of decay by an infinitely small transducer. However, in practice, shock pressures were measured at a time τ (3 and 11 μs) after reflexion using a transducer of diameter 5·6 mm.

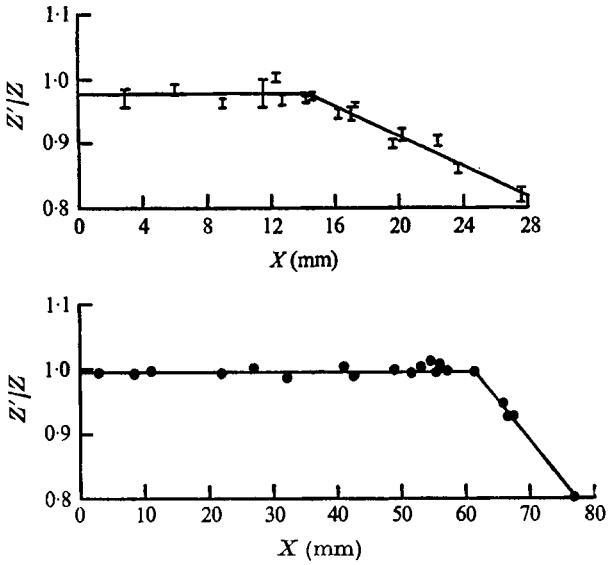

FIGURE 7. The onset of incident-shock decay. I, two dimensions, $M = 2{\cdot}18$; ●, three dimensions, $M = 1{\cdot}92$.

Number of degrees of freedom of expansion	Initial shock Mach number M	Experimental X_0 (mm)	Whitham's theory X_0 (mm)	Skews' theory X_0 (mm)	Skews' theory modified for non-ideal transducer	
					X_a (mm)	X_b (mm)
2	1·57	14·1 ± 1·0	30·6	20·1	11·3	16·1
2	1·96	15·2 ± 1·4	27·8	20·6	11·4	16·3
2	2·18	14·4 ± 1·6	27·0	21·2	11·5	16·5
3	1·55	60·3 ± 3·1	110·8	72·1	48·9	58·8
3	1·92	61·5 ± 1·8	100·4	73·8	49·4	59·5
3	2·14	60·3 ± 2·8	97·4	75·7	50·0	60·3
3	2·42	56·6 ± 5·0	95·0	78·0	50·7	61·3

TABLE 1. Correlation between experimental and theoretical positions of the onset of decay

X_0 can be modified to account for these factors by making assumptions about the way in which a pressure transducer responds as an expansion wave crosses its surface. Thus a limiting position X_a for the detection of the onset of decay is that where at a time τ after reflexion the expansion has just reached the outside edge of the pressure transducer. The values of X_a given in table 1 are limiting, because of the assumption that the pressure transducer is capable of detecting the initial and very small decrease in pressure of the shock. Owing to the scatter of the experimental results such an ideal situation does not occur. A less exacting criterion is that it is possible first to detect the pressure decrease when the head of the expansion wave has just reached the centre of the transducer. The corresponding distances X_b, where the entire surface of the transducer has been

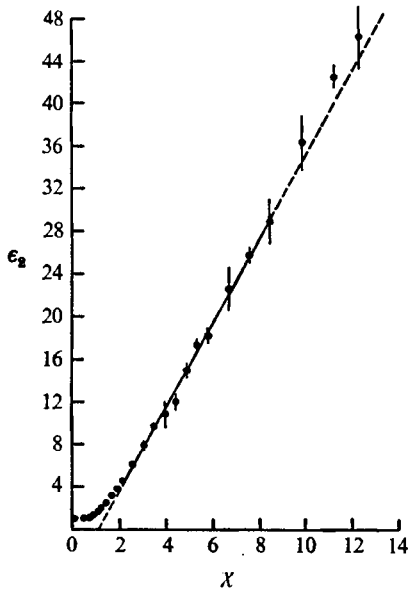

FIGURE 8. Cylindrical expansion, $M = 1{\cdot}57$.

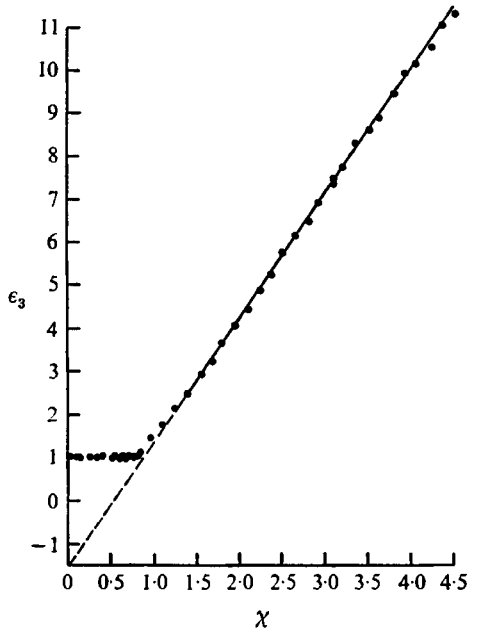

FIGURE 9. Spherical expansion, $M = 1{\cdot}92$.

affected by the expansion wave, are given in the final column of table 1. It can be seen that for two degrees of freedom the experimental distances lie comfortably between the distances X_a and X_b given by the assumptions of two extremes of transducer sensitivity. The results for the expansion with three degrees of freedom in general lie much closer to X_b, which may reflect the lower frequency response of the transducer used.

Thus differences between the experimental position of the onset of decay and the predicted position of the critical shock are accounted for by the non-ideal behaviour of the pressure transducer.

4.3. *The axial decay of the shock wave*

The experimental results were expressed in terms of ϵ_2 and ϵ_3 using

$$\epsilon_2 = f(Z)/f(Z'), \quad \epsilon_3 = (f(Z)/f(Z'))^{\frac{1}{2}}, \tag{8), (9}$$

where $f(Z)$ and $f(Z')$ are the Chisnell functions appropriate to the shock strengths of the initial and decaying shock waves. Equations (4) and (5) were tested by plotting the appropriate values of ϵ against χ. In figure 8, which shows the two-dimensional results for a Mach 1·57 shock, each vertical bar represents the standard deviation within three runs. ϵ_2 remains approximately constant at 1·0 until the critical shock position is passed, when it increases steadily to follow adequately a linear relationship for $\chi > 2{\cdot}0$. The straight line is much more striking in figure 9, which gives the three-dimensional results for a Mach 1·92 shock. The results for all the shocks studied reduce to straight lines at least up to

Number of degrees of freedom of expansion	Mach number of initial shock	Slope	ϵ intercept	χ intercept	Onset of linearity χ
2	1·57	3·96 ± 0·19	−4·37 ± 0·94	1·10 ± 0·24	2·0
2	1·96	3·11 ± 0·08	−2·17 ± 0·35	0·70 ± 0·11	1·5
2	2·18	2·79 ± 0·09	−2·05 ± 0·40	0·74 ± 0·14	1·5
3	1·55	3·15 ± 0·07	−2·12 ± 0·19	0·67 ± 0·06	1·4
3	1·92	2·84 ± 0·03	−1·58 ± 0·08	0·56 ± 0·03	1·3
3	2·14	2·54 ± 0·06	−1·10 ± 0·15	0·43 ± 0·06	1·0
3	2·42	2·62 ± 0·06	−1·27 ± 0·16	0·48 ± 0·06	1·0

TABLE 2. Least-squares analysis of ϵ *vs.* χ

$\chi = 8$ and $\chi = 4$ for the two- and three-dimensional cases respectively. The distance of the onset of linearity is given in table 2 along with data from a least-squares analysis of the lines.

The geometrical requirements of the model led to (4) and (5), which are linear if both α'/α (or θ'/θ) and $\overline{PT}$ are constant ($\overline{OQ}$ is already constant by definition). These are exactly the requirements for symmetrical expansion; i.e. the shock wave appears to propagate from a fixed point P, leading automatically to a constant angle between the ray directions.

Unfortunately, the analysis does not lead directly to values of θ'/θ, α'/α or $\overline{OQ}$ but the χ intercept does give $\overline{TP}$, the axial distance from the entrance of the area change to the point P on which the expansion is apparently centred. This point is always within the area change, and closer to the entrance for stronger shocks. The values of χ at which the results begin to obey a linear relationship indicate that a shock wave must travel further to attain cylindrical symmetry in a two-dimensional case than the corresponding shock wave with three degrees of freedom needs to travel to become spherically symmetric. Also, in general the distance that a shock has to travel to attain symmetry decreases as the initial Mach number increases.

4.4. *Three-dimensional results at* 12·7 *diameters* (1 m)

Values of ϵ_3 at 1 m from the end of the shock tube have been obtained by substituting $\chi = 12{\cdot}7$ into (4) for each initial Mach number using the appropriate parameters from the linear analysis (table 2). It should be noted that, even with the large errors ($\pm 15\,\%$) in the linear parameters, the spread in the reflected-shock pressure ratios is less than 2 %.

The experimental and predicted results are compared in figure 5, where a dashed line has been drawn through the predicted results. On this scale the spread in the predictions is small and has been omitted. As can be seen, the correlation is excellent for the two weakest shocks. For the stronger shock waves the experimental shock strengths are below those predicted. Although the correlation deteriorates as the initial Mach number increases, the predicted values of Z_r' are within 12% of those obtained by experiment.

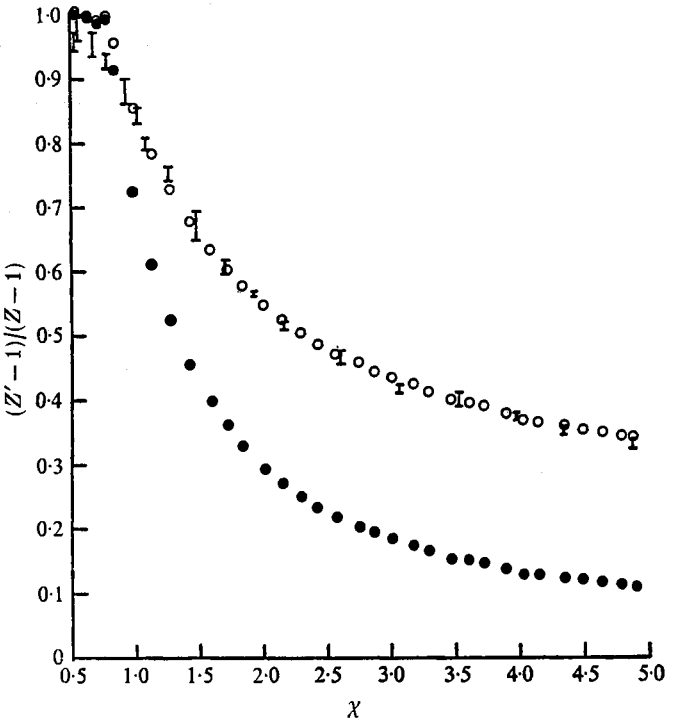

FIGURE 10. Correlation between shock expansion in two and three dimensions. ●, experimental, three dimensions; I, experimental, two dimensions; ○, predicted, two dimensions.

4.5. *Correlation between results in two and three dimensions*

The experimental values of ϵ_2 and ϵ_3 are best compared in terms of the ratio ϵ_2/ϵ_3. This quotient q was always between 1·25 and 0·85. These extreme values were obtained from the plateau region in three dimensions and in the early stages of the decay respectively. (The high value can be explained in terms of the response times of the two types of transducer used, since the transducer used for the measurements in two dimensions detected the onset of decay at a lower value of χ.) As χ increased, q rapidly approached 1·0, after which it increased slowly, so that at $\chi = 5{\cdot}0$ the maximum value of q was only 1·13.

In view of the random and systematic errors incurred in the measurements, q was approximated as 1·0 for all values of χ, leading to

$$\epsilon_3 \simeq \epsilon_2. \tag{10}$$

For values of ϵ_3, this approximation gave the corresponding values of ϵ_2 and thus the Chisnell function $f(Z')$ of the corresponding decaying shock in two dimensions. The shock strength Z' in two dimensions was obtained by iterative computation.

The experimental results from the decay of a Mach 1·92 shock in three dimensions were reduced in this way to give predicted shock strengths in two dimensions. In figure 10 these are compared with the experimental results for Mach 1·96 decay in two dimensions. The normalized incident overpressure

$(Z'-1)/(Z-1)$ was plotted, since this gave greater separation between the experimental values and the predicted results than a simple plot of the normalized shock strength Z'/Z.

For $\chi > 1{\cdot}5$ the correlation is evidently excellent, the predicted results generally lying within the experimental spread. Nearer to the area change the correlation is poorer, but is considered adequate for $\chi > 0{\cdot}9$, below which the effect of using different pressure transducers predominates. These observations are generally true, and the predicted results are in excellent agreement with the experimental results for all the shock Mach numbers for $\chi > 1{\cdot}5$. The approximation $q = 1{\cdot}0$ can be used in the reverse direction to predict three-dimensional results given the shock strengths in a two-dimensional expansion. This is of more practical use, since the apparatus required for measurements in a three-dimensional expansion is much larger and more complex. This study shows that results attained in two dimensions can readily be extrapolated to predict the corresponding shock decay in three dimensions.

5. Discussion

The model which has been developed provides a convenient method of analysing shock-strength measurements in decaying shock waves. In effect the pressure ratio Z of a shock is replaced by the function $f(Z)$ (Chisnell 1957), which is inversely proportional to the surface area of a small element of the shock close to the axis. If the surface areas of the initial and decaying shock are known, then application of (1) gives the Chisnell function $f(Z')$ of the decaying shock, which by iteration leads to the decaying pressure ratio Z'.

The surface areas are known only in the quasi-steady case of planar shocks which result from the passage of a shock through a small and gradual area change. In all other cases, approximations have to be made or empirical relationships obtained. The latter approach leads to linear relationships between ϵ and χ for the range of shock Mach numbers studied.

Ideally, values of ϵ obtained by an infinitely small pressure transducer of perfect resolution remain at unity until the critical position is reached at X_0, predicted by the use of Skews' value of α in (6) and (7). In practice ϵ is greater than unity at X_0, and this can give an estimate of the effect of using a non-ideal pressure transducer. For example, for a Mach 1·55 shock, ϵ_3 is 1·27 at X_0, and this leads to a value of the pressure ratio of the shock which is 12 % lower than that of the critical shock. Such overall systematic errors arise from two sources, and the contribution from each has been estimated (table 3).

First, the finite size of the pressure transducer means that the recorded pressure is the integrated effect of a pressure gradient across the diaphragm. The contribution of this effect is the same in two and three dimensions, but this is due to a fortuitous relationship between the dimensions of the rectangular and cylindrical shock tubes. This accounts for less than 5 % of the error and, as X is increased beyond X_0, the pressure gradient across the diaphragm decreases and the integrated pressure tends to the true axial pressure.

The second source of error arises from the delay τ in measuring the overpressure.

Two dimensions			Three dimensions		
M	Size	Time lag	M	Size	Time lag
1·57	4%	3%	1·55	4%	8%
2·18	4·5%	5%	2·14	4·5%	13%

TABLE 3. Contributions to the systematic error in Z' at the critical shock position

Obviously, since the shock wave is followed by an expansion wave, measurements made at the instant of shock reflexion would give higher pressures. As the pressure probe is moved beyond the critical shock position, the gradient of the expansion wave decreases rapidly. Hence as before the error decreases with axial distance and the delayed pressure measurement tends to the instantaneous pressure.

The net effect is that the systematic errors decrease as the probe is moved beyond the critical shock position. Since even the maximum error causes only relatively small changes in the values of ϵ, it is expected that the linear plot is a close approximation to the ideal one.

Thus it is claimed with considerable confidence that there is a linear relationship between ϵ and χ. This implies that the shock undergoes symmetrical expansion, and the ratio ϵ of the Chisnell functions is a measure of the surface areas of the decayed and critical shock waves. Now it is expected that the shock wave will eventually undergo symmetrical expansion. Therefore the observed linear dependence is evidence of the equivalence of ϵ and the area ratio. This important conclusion means that Chisnell's (1957) theory of the propagation of a shock wave through a gradual area change can be extended to include the unsteady propagation of a shock through a large and abrupt area change, but that the area of the initial shock must be defined in terms of the surface area of the critical shock.

Unfortunately, the analysis does not provide a means of determining these surface areas nor of predicting shock decay solely from a knowledge of the duct geometry. Nevertheless, considerable progress has been made towards the production of a quantitative model. For any shock with initial Mach number within the experimental range ($1{\cdot}5 < M < 2{\cdot}5$), quantitative application of the linear relationships provides the strength of the decaying shock in a two- or three-dimensional half-space. Also, when the linear relationship has been determined experimentally for any initial shock Mach number, this can be extrapolated to predict the shock strength at distances outside the experimental range.

The validity of the approximation $q = 1{\cdot}0$ provides further evidence that Chisnell's (1957) theory can be used for large abrupt area changes, and shows that the results do indeed scale in terms of χ. It is of interest to note that in a gradual area change $q = 1{\cdot}0$. Hence the geometrical relationship between cylindrically and spherically expanding shocks in gradual area changes is a reasonable approximation in the more complex situation of an abrupt area change.

6. Conclusions

(i) Chisnell's (1957) theory can be extended to include large abrupt area changes, provided that the initial area is defined in terms of the surface area of the axial segment of the critical shock.

(ii) The critical-shock model gives a realistic and quantitative description of the behaviour of a shock wave in a half-space. The results predicted by the model can be reduced to a linear relationship between ϵ and χ.

(iii) A shock wave must travel further to attain cylindrical symmetry on passing through a two-dimensional expansion than to attain spherical symmetry in a corresponding three-dimensional expansion. The apparent centre of the cylindrical symmetry is further from the entrance of the area change.

(iv) The approximation $\epsilon_2 \simeq \epsilon_3$ enables the prediction of the shock strength along the axis of a two-dimensional expansion given the corresponding results for the three-dimensional case (or vice versa).

The work was carried out at the Central Electricity Research Laboratories and is published by permission of the Central Electricity Generating Board. The authors would like to thank Mr S. Jones and Mr Y. S. Soo for their assistance with the experiments. Thanks are also due to Professor A. G. Gaydon for many helpful discussions.

REFERENCES

CHESTER, W. 1953 The propagation of shock waves in a channel of non-uniform width. *Quart. J. Mech. Appl. Math.* **6**, 440.

CHESTER, W. 1954 The quasi-cylindrical shock tube. *Phil. Mag.* **45** (7), 11293.

CHISNELL, R. F. 1957 The motion of a shock wave in a channel with applications to cylindrical and spherical shock waves. *J. Fluid Mech.* **2**, 286.

DAVIES, P. O. A. L. & GUY, T. B. 1971 Shock wave propagation in ducts with abrupt area expansions. *Symp. on Internal Flows, University of Salford*, paper 30, p. D46.

DECKKER, B. E. L. & GURURAJA, J. 1970 An investigation of shock wave behaviour in ducts with a gradual or sudden enlargement in cross-sectional area. *Thermodyn. Fluid Mech. Convention, University of Glasgow*, paper 4, p. 27. (See also *Proc. Inst. Mech. Engrs*, **184**, 3 G.)

JAMES, D. J. 1965 An investigation of a pressure wave propagated from the open end of a 30 in. × 18 in. shock tube. *A.W.R.E. Rep.* no. 0-60/65.

NETTLETON, M. A. 1973 Shock attenuation in a gradual area change. *J. Fluid Mech.* **60**, 209.

SKEWS, B. W. 1966 Profiles of diffracting shock waves. *University of Witwatersrand, Dept. Mech. Engng Rep.* no. 35.

SKEWS, B. W. 1967 The shape of a diffracting shock wave. *J. Fluid Mech.* **29**, 297.

WHITHAM, G. B. 1957 A new approach to the problems of shock dynamics. Part 1. Two-dimensional problems. *J. Fluid Mech.* **2**, 145.

WHITHAM, G. B. 1959 A new approach to the problems of shock dynamics. Part 2. Three-dimensional problems. *J. Fluid Mech.* **5**, 369.

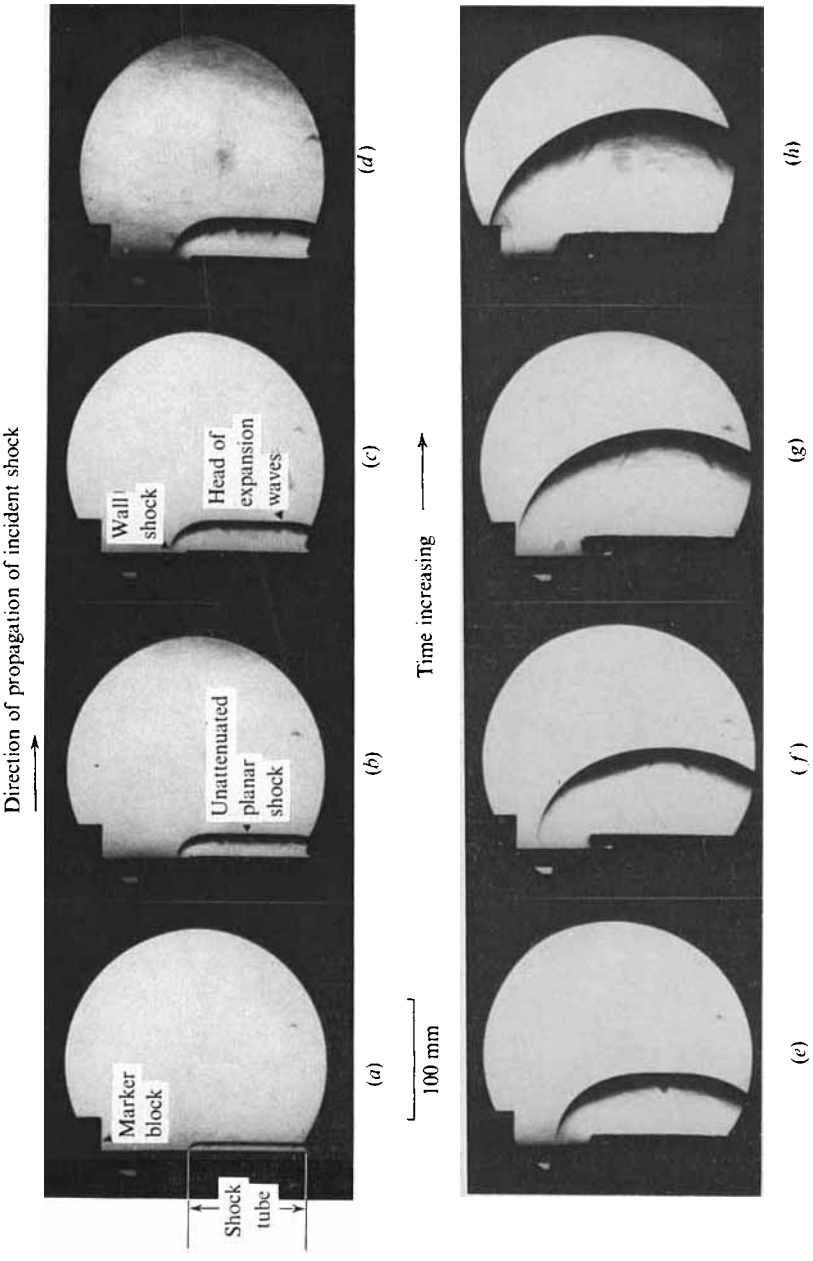

FIGURE 3. Schlieren study of a shock wave expanding in three dimensions.